



Seismic site effects investigation in the urban area of Nador (NE Morocco) using ambient noise measurements

Aboubakr Chaaoui^{1,2} · Mimoun Chourak² · José A. Peláez³ · Seif-eddine Cherif⁴

Received: 4 April 2019 / Accepted: 10 August 2021 / Published online: 2 September 2021
© Saudi Society for Geosciences 2021

Abstract

Seismic site effects are related to the local lithology, which modulates seismic waves and can enhance their amplification. For this reason, the horizontal-to-vertical ratio (H/V technique) was used to characterize them in the urban area of Nador. Ambient noise was measured at 190 different sites in order to characterize the sedimentary deposits from a seismic point of view, with further reference to 53 available geotechnical boreholes. The first investigation on site effects in Nador city, presented in this study, gives fundamental frequency values between 2.1 and 5 Hz and an amplification factor range between 2.5 and 11.4. No amplification is found in rock soils except for some small areas where weathered soils exist. The obtained results are compared with the H/V of a ground motion recorded in two stations. In general, results are in agreement and show that some areas display the phenomenon of amplification during a seismic action. The seismic vulnerability indices were also estimated, and values between 1 and 47 were obtained, indicating that the zones where the sediments overlie basaltic rocks are highly vulnerable, given the high impedance contrast. This microzonation study is a case study for the seismic risk assessment of Nador, ultimately contributing to urban planning and risk mitigation by defining suitable areas for building.

Keywords Nador urban area · Fundamental soil frequency · Amplification factor · Sediment deposits · Impedance contrast

Introduction

The Nador city is situated in the northeast of Morocco, along with the Alboran Sea (Fig. 1). It is considered a seismically active area in North Africa due to the convergence of the Eurasian and Nubian plates (Buforn et al. 2004; Koulali et al. 2011; Kariche et al. 2018). The results of the numerous studies classified the city as the moderate seismic hazardous

area in Morocco (Nakhcha et al. 2006; Peláez et al. 2007; Cherkaoui and El Hassani 2012).

The damage pattern in urban areas depends mainly on the characteristics of the earthquake, the site effect, and the vulnerability of structures. The site effects can modulate the seismic waves and therefore increase building damage, as occurred in numerous regions of the world: for instance, the 17 January 1995, the Kobe earthquake (M_w 6.9) (Esper and Tachibana 1998); 17 August 1999, Kocaeli earthquake (M_w 7.4) (Rathje et al. 2006); 17 January 1994, Northridge earthquake (M_w 6.7) (Boore et al. 2003); 19 September 1985, Mexico earthquake (M_w 8.1) (Mayoral et al. 2019); 21 May 2003, Algiers earthquake (M_w 6.8) (Hamdache et al. 2004); and 24 February 2004, Al-Hoceima earthquake (M_w 6.3) (Douiri et al. 2015).

In this context, the study of the characteristics of soil is important for assessing the seismic effect, which is a good tool to assess the seismic hazard in terms of the amplification (Horike et al. 2001; Bonnefoy-Claudet et al. 2006; Haghshenas et al. 2008; Foti et al. 2011; Parolai 2012).

The site response can be characterized by different analytical and experimental methods. Numerical calculations are based on boundary element methods and finite element

Responsible Editor: Longjun Dong

✉ Aboubakr Chaaoui
A.chaaoui@ump.ac.ma

¹ Laboratory of Applied Geosciences, Faculty of Sciences, Mohamed Premier University, Oujda, Morocco

² Department of Mechanics and Applied Mathematics, National School of Applied Sciences, Mohamed Premier University, Oujda, Morocco

³ Department of Physics, University of Jaén, Jaén, Spain

⁴ Laboratoire géoressources, géo-environnement et génie civil, Faculty of Sciences and Technologies of Marrakech, Cadi Ayyad University, Marrakech, Morocco

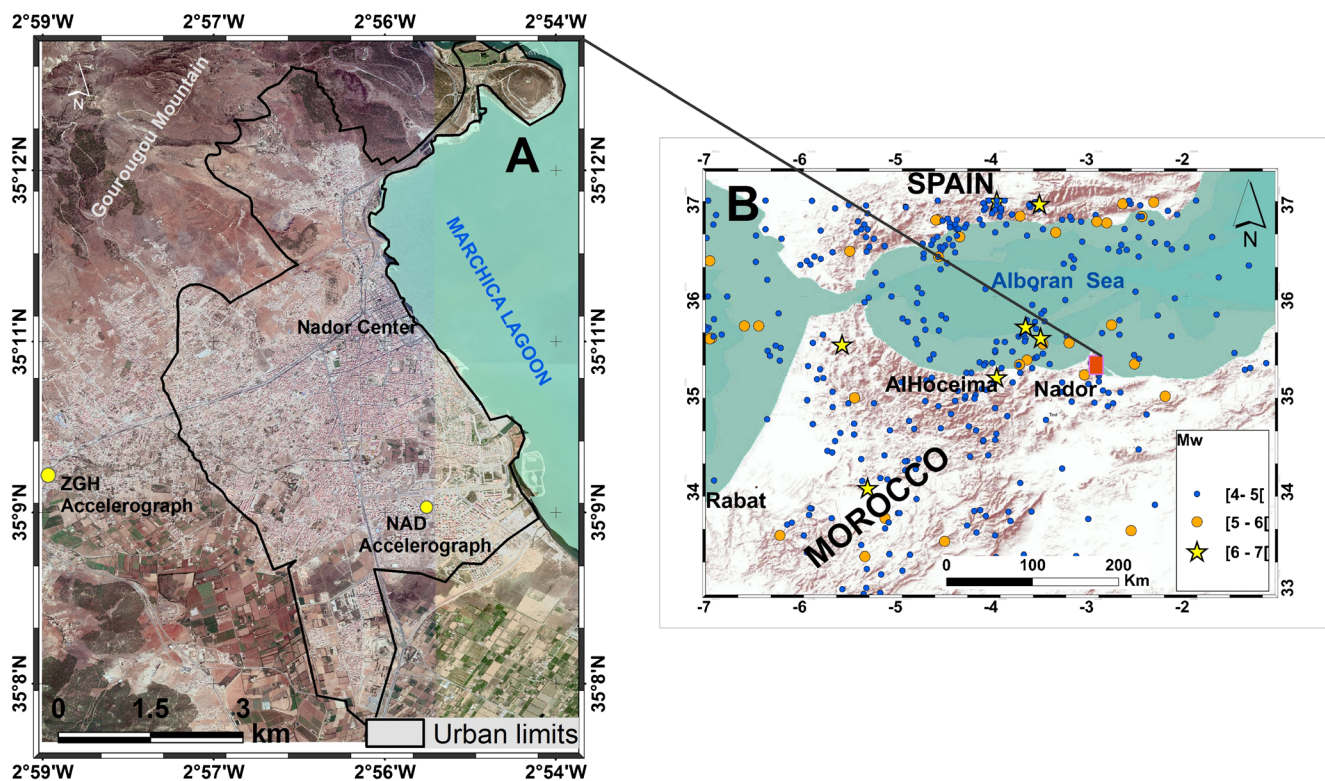


Fig. 1 A Satellite view and location of Nador city. B The nearest earthquakes since 1045 ($M_w \geq 4$) (CNRST source)

methods (Beskos 1987; Anandarajah et al. 1995; Semblat et al. 2000) adapting the analysis of waves propagation; others include the time-domain nonlinear (NL) method and the frequency-domain equivalent-linear (EQL) method (Park and Hashash 2008; Groholski et al. 2016). Site response in terms of amplification can also be determined using empirical equations by averaging the residuals between the observed and predicted peak ground acceleration (PGA) and spectral acceleration (SA) values for various periods (Douglas 2001; Campell 1981; Fukushima and Tanaka 1990). Therefore the use of ground motion prediction equation (GMPE), which is an empirical function based on earthquake characteristics (magnitude, distance from seismic source to the site, and local site conditions...) has become a very common technique to assess the site response and adopted for several studies in the world (Gulkan and Kalkan 2002; Gulkan and Kalkan 2005; Bindi et al. 2007; Ulutaş and Özer 2010; Ulutaş et al. 2011; Hamdache et al. 2019). It is important to highlight that ground motion prediction methodologies without any accounting for the source factors are inadequate. For instance, Ma et al. (2018 and 2019) concluded that ground motion values are closely related to the source focal mechanism, noting that magnitude has an exponential effect on the distribution of the PGV and PGA values. A detailed comparison of the importance of focal mechanism solution in this type of studies was also provided by Douglas et al. (2007).

On the other hand, two categories of experimental methods exist: reference site (Borcherdt 1970) and non-reference site techniques (Bard 1995). The principle of the reference site method is comparing the nearby sites records and the reference site installed on the rocky soil. The observed difference between the sites is considered due to local site effects (Jarpe et al. 1989). This technique is impractical in regions where seismic activity is low or moderate and can be applicable only to data from dense and large network stations.

In the absence of data from reference sites, techniques considering a non-reference site such as the horizontal-to-vertical (H/V) spectral ratio method are widely used to overcome this lack of data. Nogoshi and Igarashi 1970 were first to introduce this technique, and it was developed by Nakamura (1989) to estimate the site response of S waves, and it was proposed for interpreting ambient seismic noise measurements. This method was supported to determine site response for surface deposits and for microzonation studies (Lermo et al. 1994, Konno and Ohmachi 1998, Mucciarelli 1998; Strollo et al. 2011; Lachet et al. 1996; Talhaoui et al. 2004; Rosa-Cintas et al. 2017). In decades, this method has become popular for assessing local seismic responses having several advantages over other geophysical methods (seismic refraction: RF; spectral analysis of surface waves: SASW; multichannel analysis of surface waves: MASW; and refraction microtremor: ReMI...).

Many studies (Duval et al. 2001; Panou et al. 2005a, b; Pilz 2009; Clavero et al. 2017) have also used the horizontal-to-vertical ratio technique (Nakamura 1989) on ambient vibrations to determine the frequency (F_0) and the amplification factor (A_0) of ground motion so as to gauge site effects. The (F_0) of the soil and the frequency derived by the H/V technique show good consistent (Albarelo and Lunedei 2010).

The studies of seismic risk in the Rif region of Morocco demonstrated that the damage is due principally to local site amplification and type of the buildings (Talhoui et al. 2004; Douiri et al. 2015).

According to the Moroccan code (RPS 2000, revised in 2011), the Nador city is classified as an area of high seismicity in the Moroccan, with the PGA values of 0.17 g for a return period of 475 years. Intensity VII was felt in Melilla (1926) (15 km from Nador), while intensities VIII and IX were felt during Al-Hoceima earthquakes ($M_w=6.0$ and $M_w=6.4$ in 1994 and 2004, respectively). These earthquakes occurred near Nador, and they resulted a loss of lives and produced significant damage (Cherkaoui and El Hassani 2012).

Also known as “Europe’s gateway,” the city of Nador is the largest economic and touristic zone in northeastern Morocco, with a population over 565,000 (HCP 2017). The study region is classified as a biological and ecological place of interest and also as a RAMSAR site of international importance (under the RAMSAR Convention) since 2005 (Haddouti and Zerrouki 2016). It accommodates new construction and development projects (resorts, hotels, harbor, bridges, and various railway networks), mainly managed by the Agency for the Development of the Marchica Lagoon (<http://www.agencemarchica.gov.ma>).

From a geological standpoint, the Neogene Basin of Nador composed by two main units can be differentiated (Faure-Muret 1992). The first formation is situated in the Nador-Bouarg Basin, covered by deposits of recent Quaternary, formed by the sedimentary rocks (clays, silts, and sands) from alluvial, lagoon origins, and the reliefs surrounding the basin (Fig. 2). The new city of Nador lies on the Bouarg Plain, characterized by sediment deposits in the top layer. The paleo-valleys, produced by sub-aerial erosion during the Messinian, is composed by the conglomerates surmounted by marine silt and sandy marine deposits of the Plio-Quaternary (Achalhi 2016).

To the north and northwest, a massif called the Gourougou Mountain (of Tortonian to Messinian age) was formed in the wake of volcanic and tectonic events. This volcanism limits the Nador Basin, constituting the basement of the Bouarg-Nador Basin, yet it continued with the eruption of alkaline basalt within the broader framework of Eastern Rif magmatism (El Bakkali et al. 1998). The results of the seismic reflection survey, depicted in Fig. 3, show that the basement is at a depth of 740 m (Ammar et al. 2007).

The analysis of the 53 geotechnical boreholes (Fig. 2) provides the lithology and the thickness of the shallowest layers that enabled us to characterize the volcano-sedimentary sequences in the Nador region.

We classified the different types of soils into three categories (Fig. 4):

The soft sediments with the thickness up to 40 m compose the category (a). These soft soils are mainly fluvial and littoral sediments susceptible to liquefaction due to the high compressibility of the clay and limestone (Youd and Perkins 1978; Delgado et al. 1998). These sediments have a shear wave velocity (V_s) ranging from 100 to 500 m/s. The area near Azougagh River contains significant sediment infill of recent accumulation.

The category (b), found near the Gourougou Mountain, comprises two layers. The shallow layer is formed by sedimentary rocks (clay and sandy clay colluvium) whose thickness varies between 4 and 8 m, derived from the geotechnical boreholes. The volcanic rocks and basalts constitute the second layer. The origin and the properties of the two layers are totally different, especially in terms of density, reflected by the impedance contrast between the sediments and the hard bed rocks (Narayan 2010).

The category (c), located in the west and northwest part of the basin, is composed by a volcanic substratum. This unit exists in the mountainous part, very dense, and the V_s is greater than 760 m/s (RPS 2000).

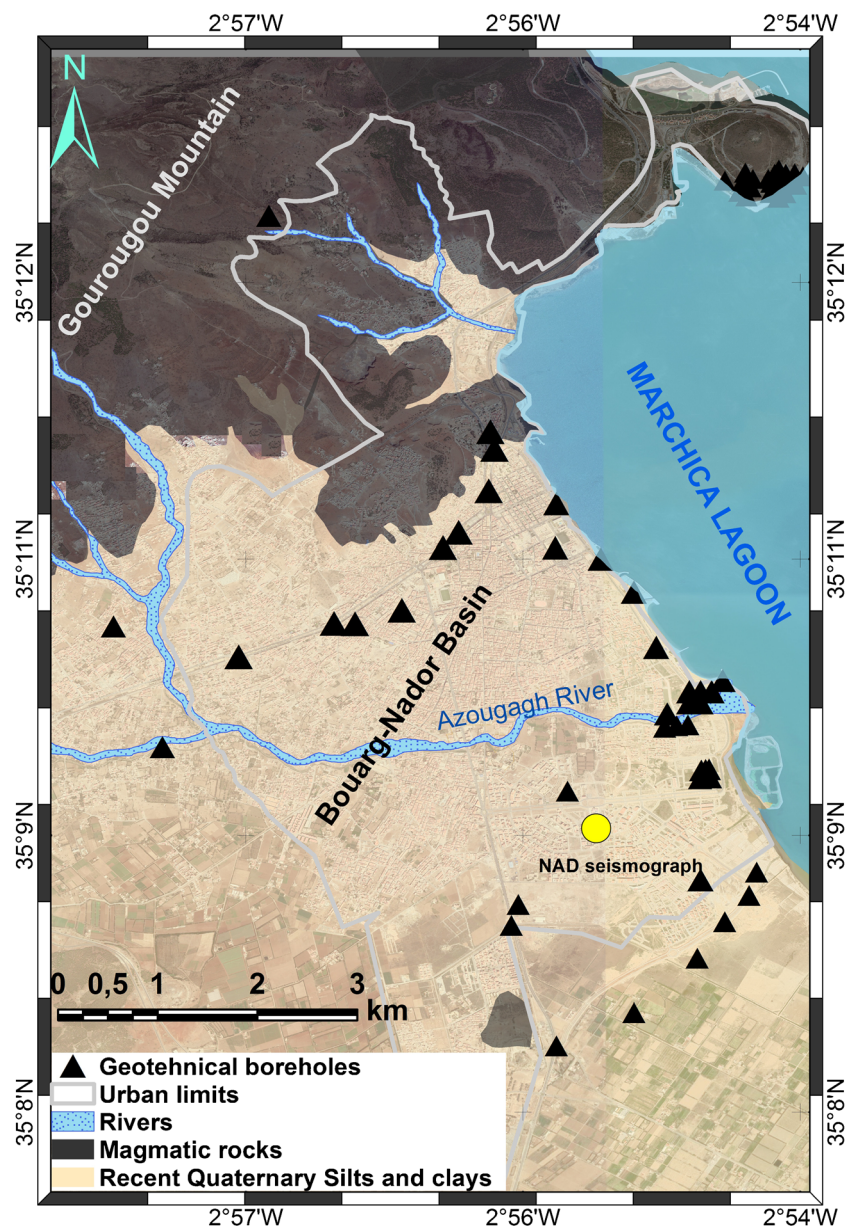
The present study, focusing on the urban area of Nador, improves upon the soil classification proposed by Moroccan seismic code (RPS 2000), arriving at an estimation of site effects based on ambient vibrations, earthquake records, and geotechnical boreholes in the region.

Data and methodology

H/V technique to characterize site response

The horizontal-to-vertical ratio (H/V) technique using spectral ratios of ambient vibration data is widely applied for microzonation studies (Mubin and Nurcahya 2014, Lachet et al. 1996, Panou et al. 2005a, b, Talhoui et al. 2003, Parolai 2012; Poggi and Fäh 2016; Ali and Kim 2016; Rosa-Cintas et al. 2017). This passive technique was introduced by Nogoshi and Igarashi (1970) and developed by Nakamura in 1989 (Nakamura 1989), who introduced the spectral ratio between the horizontal and vertical components of ambient noise recordings, at different frequencies, in the study area. Two explanations have been proposed regarding the origin of ambient noise. Nakamura (1989) claims that the horizontal-to-vertical spectral ratio (HVSr) mainly reflects S-wave resonance in the soft surface layers, providing the estimation of site amplification.

Fig. 2 Map of the main geological units of the study area and spatial distribution of the geotechnical boreholes available around



Nakamura's interpretation has been contradicted by studies relating the spectral ratio to the ellipticity of Rayleigh waves (Bard 1998). Both interpretations, however, confirm that the technique captures the relationship between fundamental frequency and soil depth and is therefore useful for site response evaluation (Lermo et al. 1994) and reliable assessment of ground motion characteristics in soft sediment soils (Mucciarelli and Gallipoli 2004; Zaslavsky et al. 2008). The advantages of this method are its low cost, fast survey performance, and adequacy for urban areas, not requiring earthquake data (Lermo et al. 1994; Duval et al. 2001; Panou et al. 2005a, b; Mucciarelli 2008; Parolai 2012).

In essence, this method records ambient vibrations in two orthogonal-horizontal directions plus the vertical one. Analysis entails computing the Fourier spectrum for each

signal, after which the different signals are processed to obtain an equivalent spectrum, with a peak corresponding to the fundamental frequency (F_0) of the soil according to a given amplification (A_0). The resulting amplification is underestimated, however (Lachet et al. 1996; Strollo et al. 2011) not necessarily coinciding with the ground amplification level obtained from earthquake records (Bonilla et al. 1997; Horike et al. 2001; Satoh et al. 2001).

Data acquisition and processing

For the purpose of this experiment, 190 background noise recordings were conducted in the urban center and area surrounding Nador town during the period September 2016 to August 2018. Ambient vibrations were recorded using three

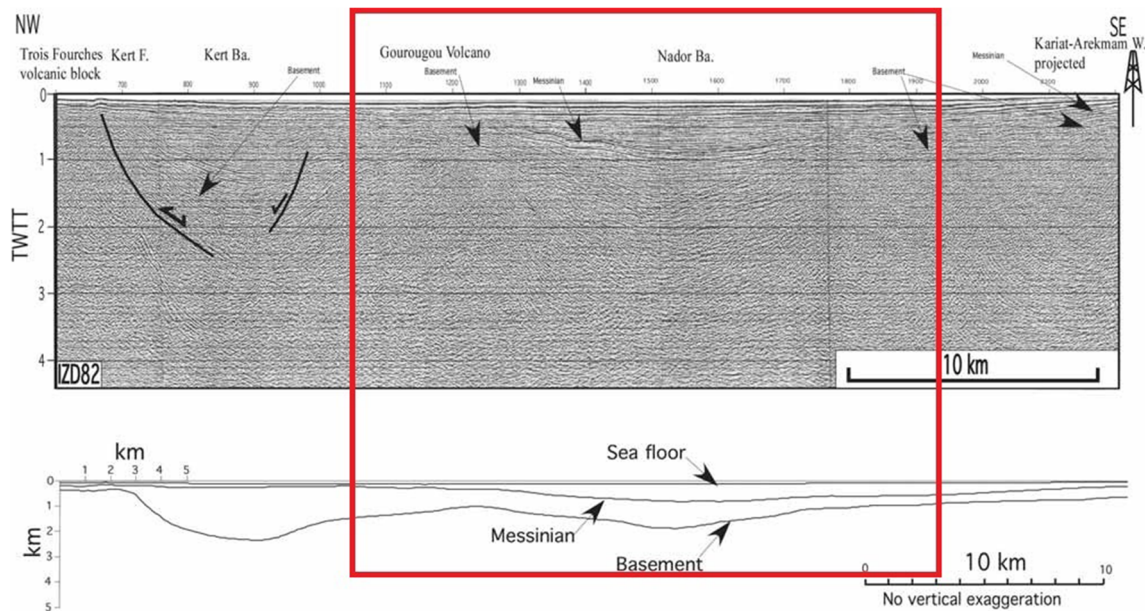


Fig. 3 Cross section obtained by deep seismic reflection in the Gourougou complex and the Nador Basin (Ammar et al. 2007)

component CMG-6TD seismometers (Guralp Systems 2017) and a laptop with the software SCREAM 4.6, allowing for visualization of the records in the field and pre-treatment and verification in situ to ensure a correct recording.

The location of measurement is selected considering the lithology, satellite images, and in the vicinity of the geotechnical drillings around the urban center. The distance between the measurement sites is ranging from 23 to 70 m and the recording time from 45 to 60 min for most sites. The geopsy software is carried out to H/V analysis. We use band pass filter in order to filter the recorded noises between 0.2 and 20Hz. We erase the time windows containing transients using the anti-triggering algorithm option; temporal windows of 25 s were selected, as well as short-term average (STA) and long-term average (LTA) window durations of 2 and 30 s, respectively. The H/V spectrum was calculated by dividing the root mean square of the Fourier amplitude spectrum of the horizontal components (F_{NS} and F_{EW}) by the vertical component spectrum (F_z) as shown in Eq. (1) (Delgado et al. 2000). Konno and Ohmachi smoothing was also used, to achieve

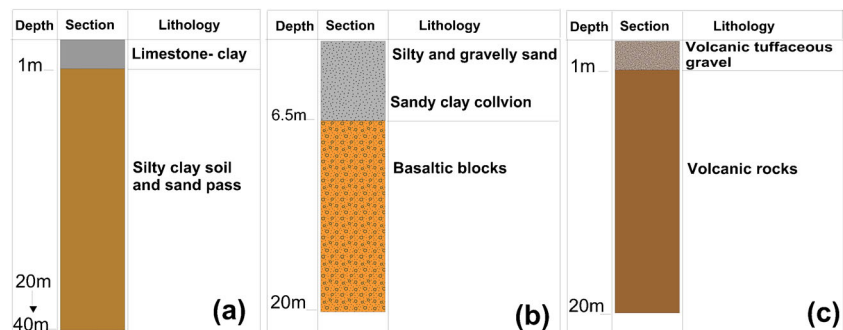
clear spectrum peaks (Konno and Ohmachi 1998).

$$H/V = \frac{\sqrt{F_{NS}^2 + F_{EW}^2}}{2F_z} \tag{1}$$

The identification of reliable H/V curves and H/V peaks was done following the guidelines of the SESAME European Research Project (Bard et al. 2004). The requirement for reliable H/V curves primarily depends on having a significant number of cycles and a large number of measurement windows. The condition $F_0 > 10/l_w$ must be satisfied, where F_0 is the fundamental frequency and l_w the window length. The total number of significant cycles n_c should be larger than 200 with $n_c = l_w \cdot n_w \cdot F_0$, where n_w is the number of windows. The verification of the reliability of the H/V peak is also performed considering the following requirements (Bard et al. 2004):

- The H/V peak amplitude must be higher than 2 ($A_0 > 2$).
- There exists $F^- \in [F_0/4, F_0] \mid A_{H/V}(F^-) < A_0/2$ (F^- = frequency between $F_0/4$ and F_0).

Fig. 4 The three different types of stratigraphic columns obtained from the geotechnical boreholes



- There exists F^+ in $[F_0, 4F_0]$ | $A_{H/V}(F^+) < A_0/2$ (F^+ = frequency between F_0 and $4F_0$).
- $F_{\text{peak}}[A_{H/V}(F) \pm \sigma_A(F)] = F_0 \pm 5\%$, ($\sigma_A(F)$ is the factor by which the mean $A_{H/V}(F)$ curve should be multiplied or divided, $A_{H/V}(F)$ represents the maximum H/V amplitude of each selected individual window, and the standard deviation σ_F of H/V peak frequency estimates from individual windows.
- $\sigma_F > \varepsilon(F_0)$ ($\varepsilon(F_0)$ is the threshold value for the stability $\sigma_F > \varepsilon(F_0)$).
- $\sigma_A(F_0) > \theta(F_0)$; [$\theta(F_0)$ is the threshold value for the stability condition $\sigma_A(F) > \theta(F_0)$].

Also, recommendation is to take into account the conditions of stability and reproducibility related to anthropic and weather conditions during H/V measurements. The stability of the measurements in this study was confirmed by repeated measurements at the same place and on different dates (September 2016 to August 2018); the obtained average frequency must be identical at the same site at different times.

Results and discussion

The site responses were measured at 190 sites in the urban area of Nador (Fig. 5). The measurements confirmed by criteria for the clarity and reliability of the H/V peak (Bard et al. 2004) and clearly exhibiting peak amplification ($A_0 \geq 2.5$) were considered representative, in this case just 30% of the H/V measurements (Table 1 and Fig. 5). The rest of the H/V curves did not show any clear amplification, and the spectra are represented by flat curves with a very low amplification (Figs. 6 and 7), and therefore these measurements are not considered. The absence of clear H/V peaks is due to the fact that Quaternary sediments are heavily compacted in these areas. Furthermore, flatness or very low H/V amplitude is considered to indicate an absence of large effects, leading to a slight underestimation of the real amplification (Haghshenas et al. 2008). Our suggestion is to not consider resonance frequency from such peaks unless additional information is available (earthquake data, shear wave velocity, etc.).

For H/V curves exhibiting amplification, we noted the presence of a single H/V peak. The fundamental frequency values of H/V spectrum range from 2.1 to 5 Hz. In the west, we found values above 3 Hz, although as we move to the relief even the depth of soft sediments decreases. Most of F_0 values between 2 and 3 Hz (40 sites) are located in the northern part of the Azougagh river, representing silt-loamy soil. We correlated the presence of the predominant H/V peak with the existence of sedimentary rocks and of loose materials, i.e., silt and clays. Figs. 7 and 8 a and b present the results classified in light of the different types of curves and frequency values obtained.

Fundamental frequencies

The fundamental frequencies values obtained are depicted in Fig. 9. Values are ranging between 2.1 and 5 Hz, approximately. The fundamental frequency values describe the surface lithology, which is covered by loose sands, limestone, and sandy clay materials. Borehole in sediment layer shows the thickness of silts and clays to be over 40 m near the shoreline; it decreases as we move away to the west and to the Gourougou Mountain. Large fundamental frequency values, between 3.6 and 5.0 Hz, explain the decrease in sediment thickness, following the relationship (Nakamura 2008):

$$F_0 = \frac{V_s}{4H} \quad (2)$$

where V_s is the average shear wave velocity (m/s) and H is the sediment thickness.

Around Azougagh River, the existence of different sediments (alluvial, colluvium, and marine sediments) makes comparison difficult. We observe low fundamental frequency values on the eastern part (near the lagoon). These values increase gradually toward the west, along the Azougagh River. The same formation contains a large range of frequency values, and different peaks can be distinguished, possibly owing to the complex geological setting. Recently, large fundamental frequency ranges have been reported in different studies, e.g., from 0.27 to 3.7 Hz in Málaga city (Clavero et al. 2017) and from 0.5 to 8 Hz in Blida (Bouchelouh et al. 2017), in the similar geological formations.

Soil structure resonance is obtained by taking the frequency of the structure closest to the frequency of the supporting soil (Takewaki 1998). This finding, derived from observation of past earthquakes, is analogous to the similarity between the natural period of a building and that of the supporting soil, which was linked to significant response amplifications on buildings and serious damage in Mexico, 1985. That is, the phenomenon sheds light on the relationship between the characteristics of structure and soil and can be represented by modifying the dynamic properties of the building.

An empirical expression for estimating the natural periods for RC buildings under the Moroccan seismic code (RPS 2000, revised in 2011) is the following:

$$T = 0.075 H^1 \quad (3)$$

where T being the natural period of building and H is the building height.

The outstanding buildings within Nador vary in height from 4 to 22 m (i.e., from 1 to 7 floors). The natural periods for RC buildings must be included in the range 0.2–0.8 s, approximately. The comparison between

Table 1 Results obtained for sites showing a clear amplification

Site no.	Latitude	Longitude	Altitude (m)	Fundamental frequency F_0 (Hz)	H/V peak amplitude (A_0)	Vulnerability index (K_g)	Period (s)
6	35.1365	-2.9306	8	2.8	5.0	8.8	0.36
7	35.1369	-2.9250	9	3.2	4.0	5.0	0.31
12	35.1419	-2.9411	11	2.8	5.6	11.0	0.35
18	35.1511	-2.9467	19	2.8	7.8	22.0	0.36
19	35.1515	-2.9441	18	3.1	3.8	4.7	0.33
36	35.1566	-2.9487	21	2.8	6.1	13.5	0.36
41	35.1662	-2.9451	2	2.8	8.6	26.4	0.36
42	35.1606	-2.9510	25	2.7	7.2	19.2	0.37
43	35.1627	-2.9402	22	2.8	6.8	16.6	0.36
58	35.1613	-2.9463	28	3.1	3.9	4.9	0.32
60	35.1691	-2.9570	40	2.8	9.6	33.2	0.36
62	35.1709	-2.9399	34	3.5	3.0	2.6	0.28
63	35.1721	-2.9343	24	2.8	10.8	41.4	0.35
67	35.1822	-2.9259	8	3.4	5.0	7.5	0.30
70	35.1794	-2.9388	65	2.9	6.0	12.6	0.35
79	35.1918	-2.9330	42	2.9	5.6	11.1	0.35
84	35.1959	-2.9375	50	2.8	8.9	28.3	0.36
87	35.1982	-2.9416	69	2.8	11.0	44.0	0.36
89	35.1980	-2.9369	16	3.3	4.0	4.8	0.30
92	35.2002	-2.9281	47	2.8	11.4	47.1	0.36
93	35.2029	-2.9452	98	2.9	8.9	27.8	0.35
99	35.2143	-2.9010	37	2.8	7.8	21.8	0.36
100	35.2097	-2.9046	28	2.1	4.9	11.5	0.48
102	35.2091	-2.9023	22	2.5	4.7	8.8	0.39
113	35.1706	-2.9190	2	2.8	5.1	9.5	0.36
133	35.1540	-2.9440	21	4.3	8.0	15.0	0.23
134	35.1570	-2.9260	15	3.7	4.4	5.1	0.27
135	35.1570	-2.9220	12	2.7	9.2	31.2	0.37
139	35.1660	-2.9420	24	2.8	9.0	29.3	0.36
140	35.1640	-2.9480	28	2.7	10.0	37.6	0.38
141	35.1740	-2.9410	42	3.1	3.3	3.4	0.32
144	35.1840	-2.9250	2	2.6	4.2	6.8	0.38
146	35.1990	-2.9270	11	2.8	4.2	6.3	0.36
148	35.146	-2.942	19	2.7	6.7	16.4	0.37
149	35.149	-2.941	17	2.7	7.0	18.0	0.37
150	35.153	-2.94	14	2.7	7.0	18.3	0.37
152	35.153	-2.932	9	4.8	2.5	1.3	0.21
154	35.1770	-2.9370	22	2.7	4.1	6.3	0.37
157	35.163	-2.943	21	2.6	6.4	16.0	0.39
161	35.16	-2.942	23	2.8	8.1	23.5	0.36
162	35.163	-2.954	28	2.9	9.4	30.5	0.34
164	35.168	-2.915	2	2.8	6.9	16.8	0.35
167	35.163	-2.915	5	2.7	9.0	30.1	0.37
168	35.165	-2.939	11	2.5	3.8	5.6	0.40
172	35.162	-2.912	3	2.7	6.8	16.9	0.37
173	35.174	-2.937	18	2.8	10.1	36.1	0.35
174	35.176	-2.942	28	2.6	8.2	25.8	0.38
175	35.162	-2.92	9	2.7	6.3	15.0	0.37
178	35.17	-2.943	17	3.1	4.0	5.1	0.32

Table 1 (continued)

Site no.	Latitude	Longitude	Altitude (m)	Fundamental frequency F_0 (Hz)	H/V peak amplitude (A_0)	Vulnerability index (K_g)	Period (s)
179	35.168	-2.947	17	2.7	4.0	5.7	0.37
181	35.182	-2.944	25	2.8	10.0	35.7	0.36
182	35.173	-2.944	23	4.0	3.3	2.6	0.25
190	35.169	-2.936	14	3.1	3.8	4.6	0.32
NAD st	35.151	-2.919	7	2.8	8.0	22.9	0.36

predominant periods obtained from ambient noises and natural periods of buildings present a juxtaposition of values—ranging between 0.2 and 0.5 s—that could

produce resonance soil-structure phenomena during a seismic action. This means that buildings ranging from 1 to 3–4 floors are the most vulnerable to damage by

Fig. 5 Measurement sites

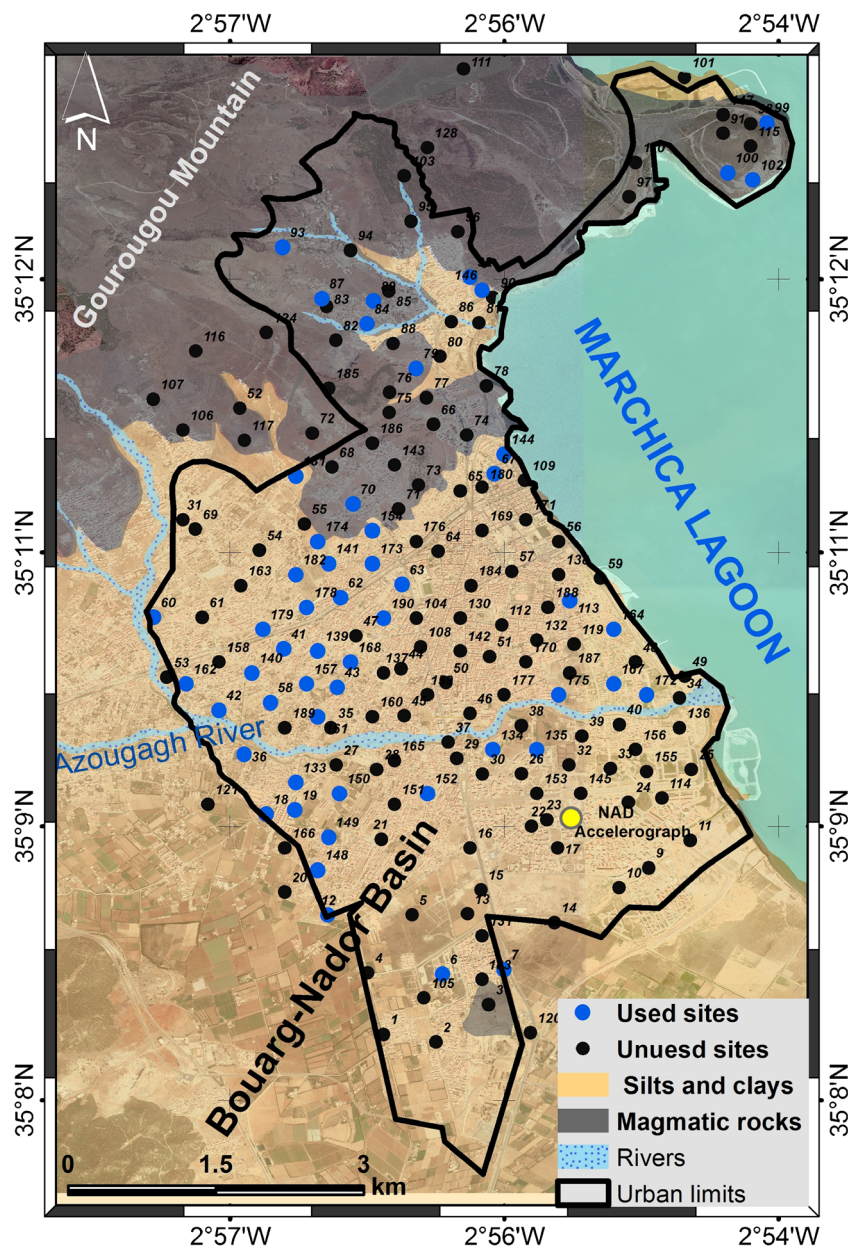
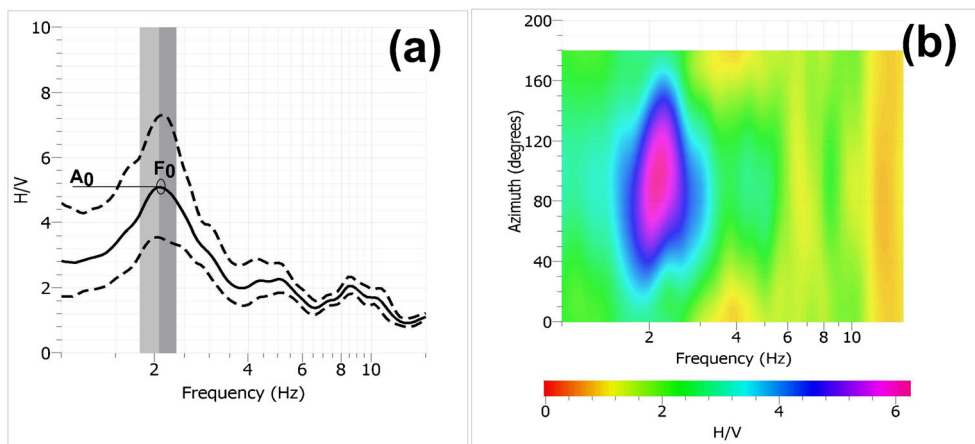


Fig. 6 H/V results (P100). **a** H/V spectral ratio; **b** vertical column is the peak frequency and std deviation around peak. Amplitude represented by the black line and the std

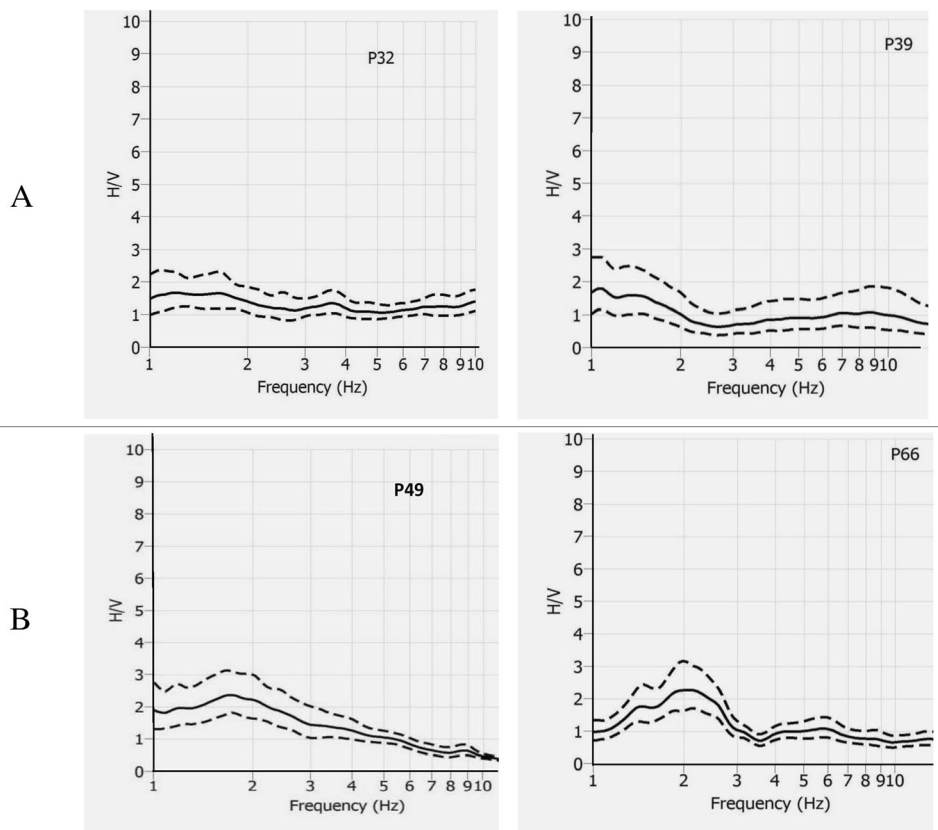


earthquakes. Such information is vital for engineers and urban designers: buildings should be designed so that the period of the structure does not coincide with the predominant period of the underlying soil.

Amplification factor

Based on the amplification results, the values can be classified in two categories (Fig. 10).

Fig. 7 **A** Examples of flat curves. **B** Examples of non-clear peaks. Locations of measurements are shown in Fig.5. The average amplitude is represented by the black



Type I: places with significant amplification (> 4.0) They correspond to resonance frequencies in the range between 2.1 and 4.3 Hz. The highest amplification factor is equal to 11.4, at site P92.

Most of these sites are located westward, in areas containing basalt under the soft sediment, as can be seen through the nearby geotechnical boreholes (Fig. 2).

Clear H/V peaks with higher amplification values correlate with important contrasts between the soil layer and bedrock

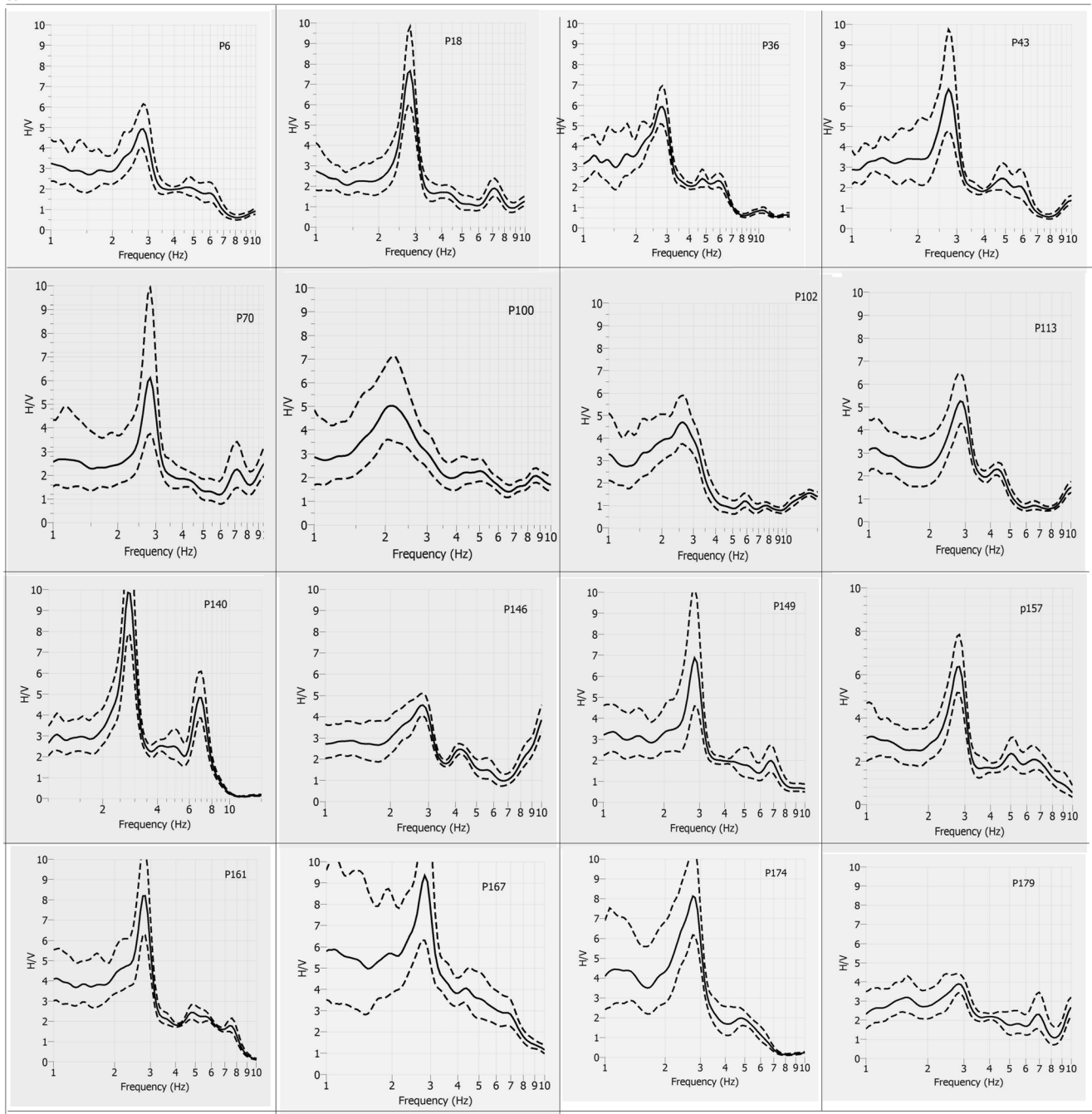
a

Fig. 8 a Main types of clear peak with frequency ranging from 2 to 3 Hz. The average amplitude is represented by the black line and **b** main types of clear peak with large frequencies, from 3 to 5 Hz. Locations of measurements are shown in Fig.5. The average amplitude is represented by the black

(Bard 1999). Certain places, e.g., P84, P93, P99, and P100, situated in areas classified as hard rock, also show significant amplification. Field observations at these sites confirm the presence of weathered soils or the existence of old quarries overlying the volcanic substratum (Fig. 12). This implies that, in addition to substratum characteristics, the lithological classification, and thickness of the sediment, it is important to

appraise local site conditions regarding the presence or absence of weathered soils.

Type II: places with low amplification: $2.5 < A_0 \leq 4.0$ These amplification levels are observed in 10 sites (including P152, P182, and P190) (Fig. 11). Almost all lie west of the city, where colluvium and gravel are found. Thin sedimentary

b

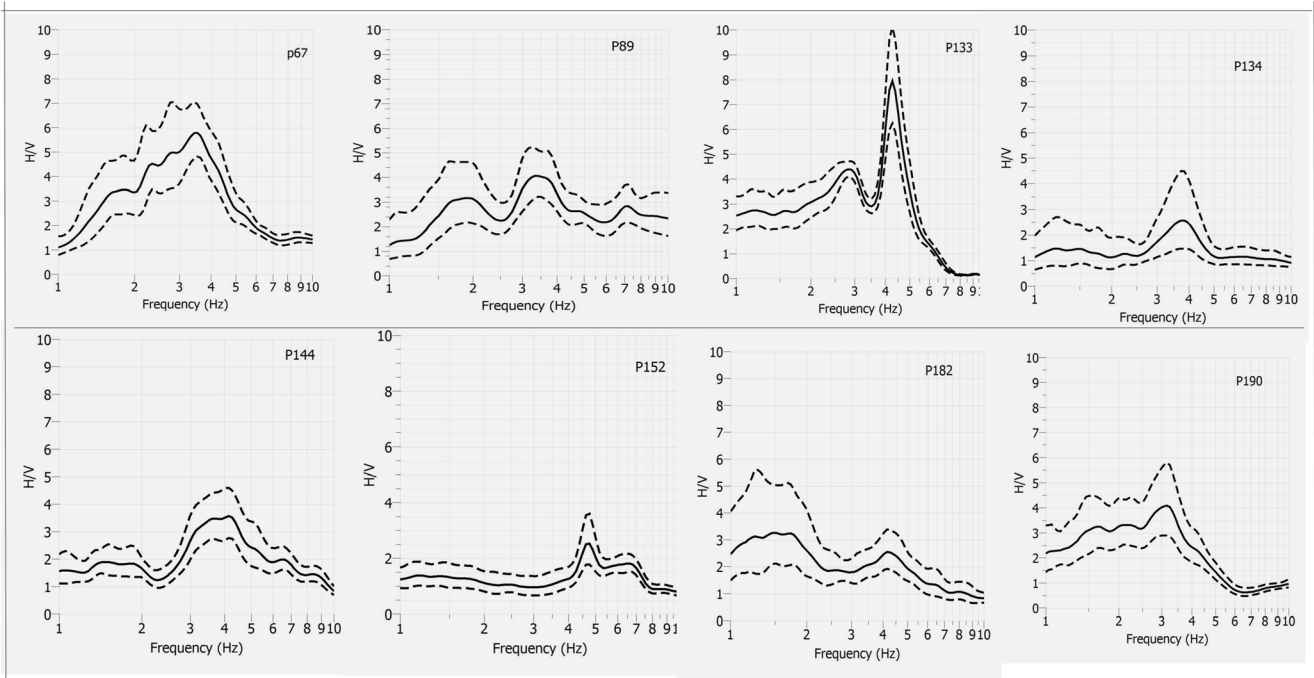


Fig. 8 continued.

layers characterize these sites. The H/V curves are more or less flat, with low amplification at certain frequencies. Large fundamental frequencies are obtained mainly in this category.

Fig. 13 gives the observed amplification factors as a function of frequency. No clear correlation is observed between the frequency and the amplitude. Altogether, 83% of frequencies with higher amplification values range roughly between 2.5 and 3.0 Hz; this interval of fundamental frequencies contains widely disperse amplification results, reaching values close to 12. Outside the range 2.5–3.0 Hz, with the exception of two sites having a fundamental frequency equal to 4.3, amplification is not high.

Seismic vulnerability indices

The seismic vulnerability index (K_g) estimates the susceptibility of a layer to deformation (Daryono et al. 2009). This parameter is given by the formula (Nakamura 1997):

$$K_g = \frac{A_0^2}{F_0} \tag{4}$$

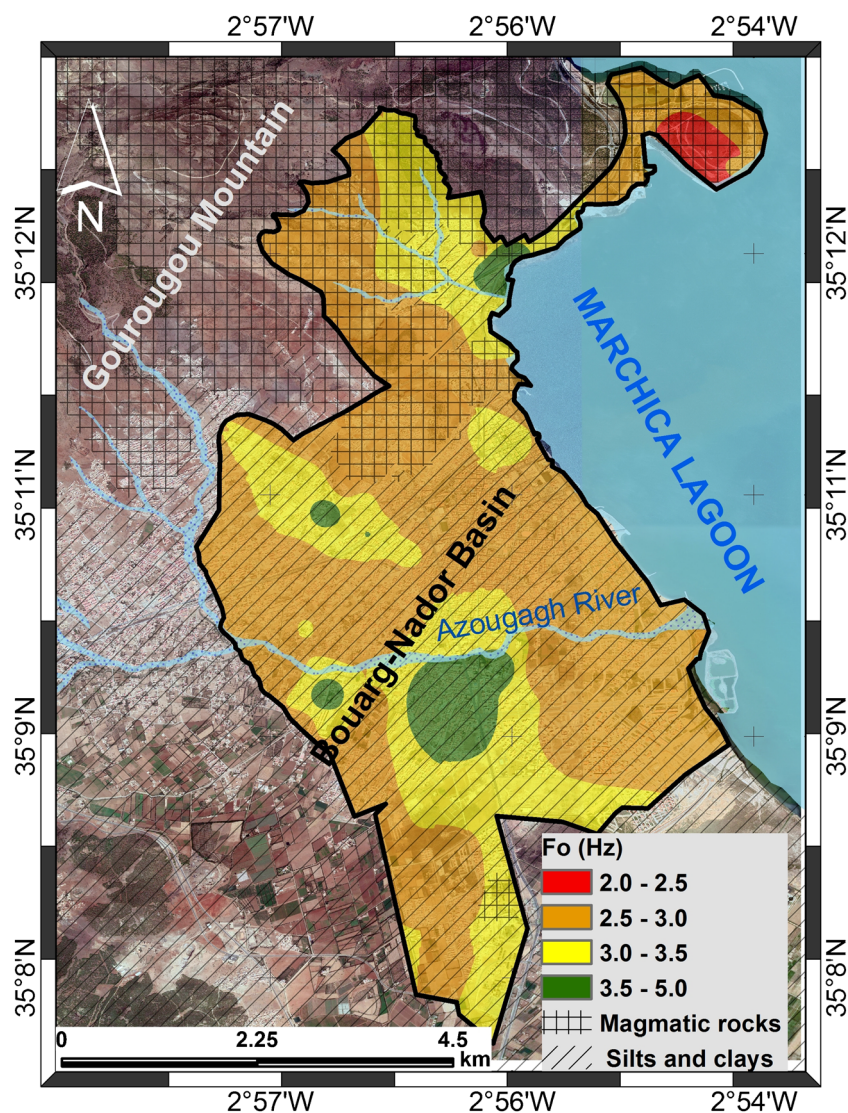
where A_0 being the amplification factor and F_0 the fundamental frequency.

Previous studies (Daryono et al. 2009; Mubin and Nurcahya 2014; Livaoğlu et al 2017) show a good correlation

between the seismic vulnerability of soil and the distribution of damage caused by an earthquake. The K_g index is very helpful for identifying areas considered to be weak zones during strong ground motions (Sunaryo 2017). Nakamura (1997) also proposed this index to quantify the vulnerability of soil to liquefaction. Determining the K_g values is potentially useful to quickly appraise the soil deformation susceptibility of surface ground by means of microtremors. Nakamura (2008) states that areas with K_g values above 20 are exposed to major damage tied to soil deformation.

The values of this parameter, as computed in this study, are presented in Fig. 14, revealing some vulnerable zones. Out of 53 values, the maximum K_g is found at site P92 in the northern part of the city. This region is covered by colluviums at the foot of Gourougou Mountain. The distribution of K_g values in Nador is irregular, even within the same quaternary sediments. Most high K_g values (>20) were found west of the city, an area characterized by high amplitude, whereas other sites having values under 20 may be found near the coast or rivers, or in the mountains. Such areas may generate less damage. Differences in the obtained values may be related to irregularities of the lithology and the existence of weathered soils and diverse sedimentary deposits of river or lagoon origin. Moreover, the geotechnical properties of each site (thickness, density, fractured rocks...) contribute to this variation. The obtained K_g

Fig. 9 Distribution of the fundamental frequency (F_0)



values show that the town of Nador could suffer potential damage due to soil deformation in certain areas.

Alboran Sea, 2016: a strong ground motion record

The National Center for Scientific and Technical Research of Morocco (CNRST) handles two accelerometric stations in Nador. One station (NAD) is located in the area of the present study (soft soil), whereas the second one (ZGH) is located on the substratum (hard rock) (Fig. 1). They recorded the ground motion during the (25 January 2016) M_W 6.3 Al-Hoceima earthquake. This earthquake was the largest event recorded in the region over the past decade, originating some 90–100 km away from Nador. Depicted in Fig. 15 are the acceleration records of the two nearby stations.

The maximum acceleration values recorded were 20.0, 47.0, and 34.9 cm/s^2 for the NAD station and 50.5, 54.4, and 61.9 cm/s^2 for the ZGH station, respectively, for the V, NS, and EW components. The durations of the signals from the Husid plot are 21.2 and 16.1 s, respectively, for the NAD and ZGH stations. The longer duration in the NAD station as compared with the ZGH station could be attributed to the dispersion and the multipath propagation between the source and the basin (Singh and Ordaz 1993; Shapiro et al. 1997; Iida and Kawase 2004), which implies that the basin of Nador could involve greater amplification than Zeghanghan (nearest city).

The predominant frequency obtained from the coda of earthquake motions showed a better correlation with microtremors than other parts of earthquake records (Upadhayay and Mori 2013). We used the coda wave from

Fig. 10 H/V amplitude (A_0) results

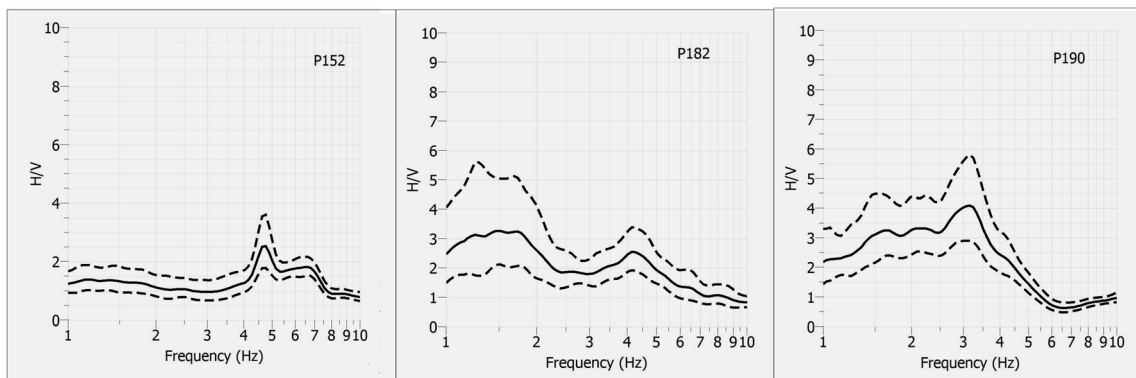
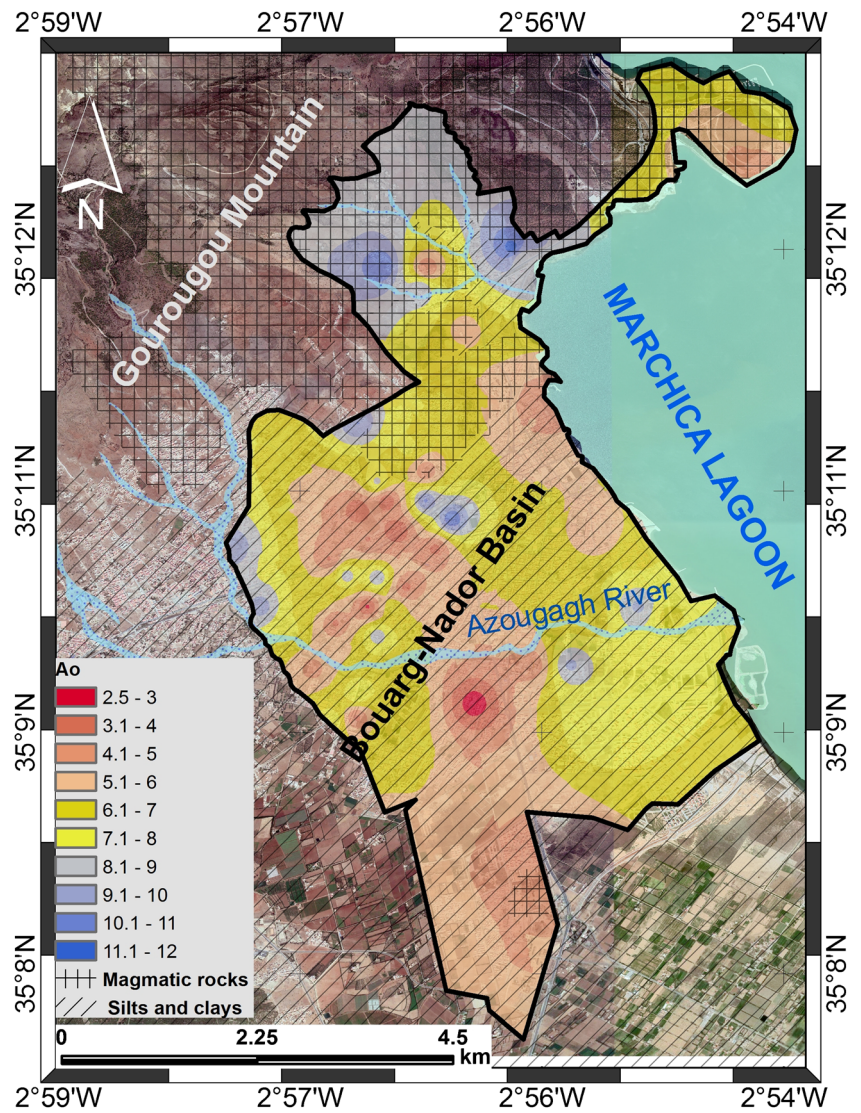


Fig. 11 Types of H/V curves exhibiting low amplification: $2.5 < A_0 \leq 4.0$. The average amplitude is represented by the black line and the standard deviation by dashed lines

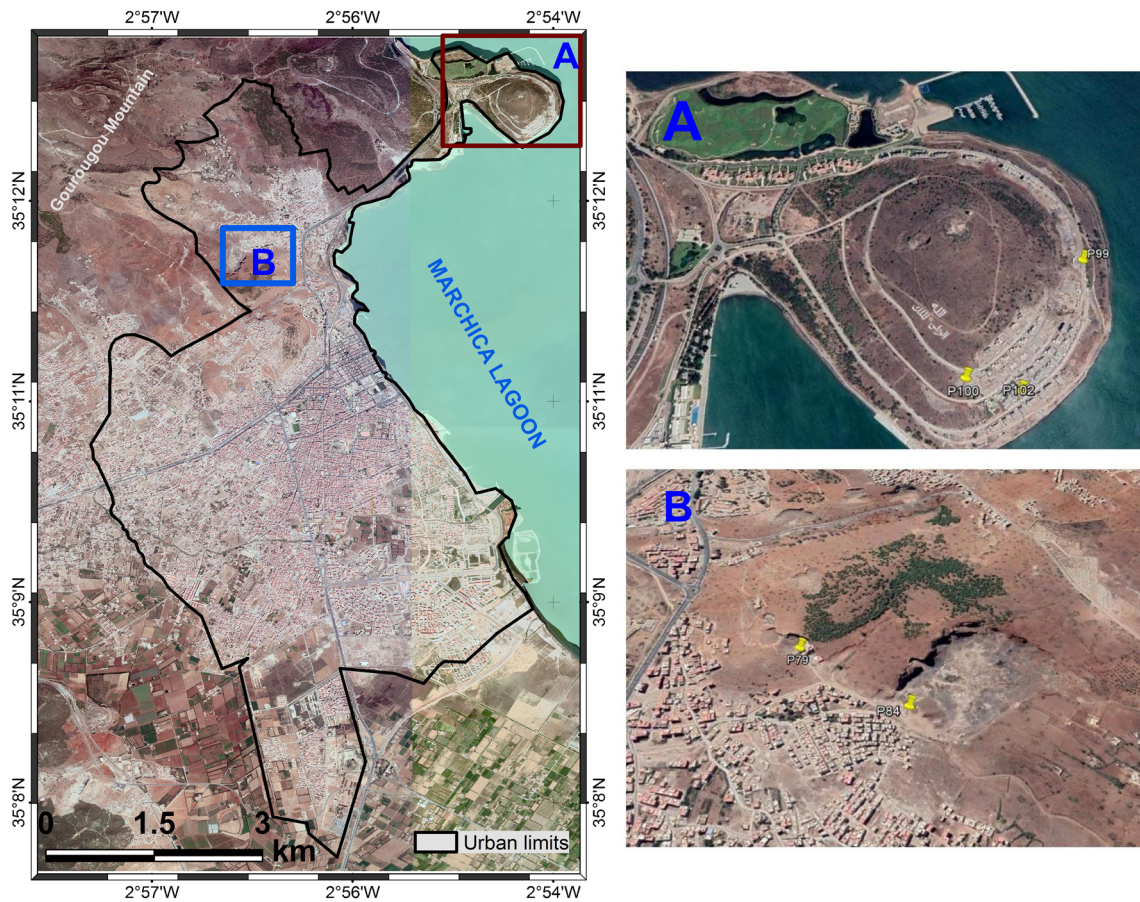


Fig. 12 Weathered soil and old carry overlying the volcanic

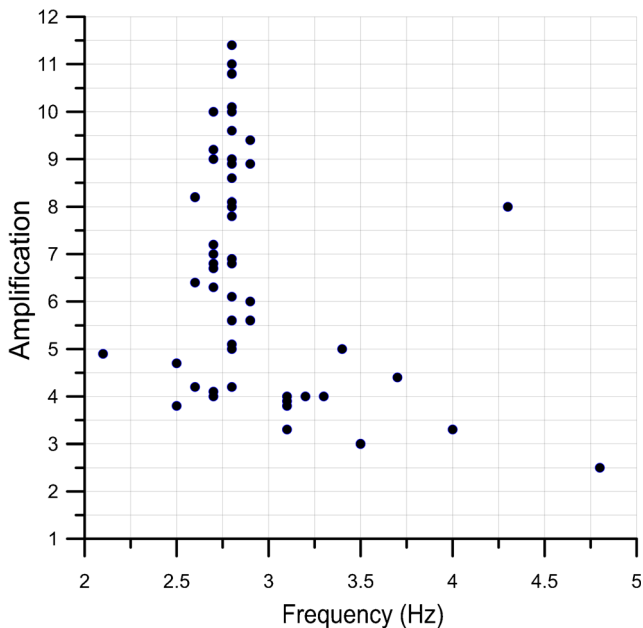


Fig. 13 Observed amplification factors as a function of fundamental frequency

the strong motion signal to process the H/V curves, likewise using Geopsy software, applying the same parameters as in the microtremor measurements—with the exception of the temporal window—in order to obtain a representative spectrum.

As seen in Fig. 16, the H/V spectrum in NAD station shows a sharp and clear peak, the fundamental frequency being 2.6 Hz, with amplification near 8. The station is located in Quaternary soft sediments. The processing performed on the rocky site (ZGH station) shows an H/V spectral ratio featuring an absence of amplification peaks.

The H/V curve from the ambient noise recorded close to the NAD seismic station at site 135 was compared with results in the NAD record (Fig. 17). Very similar results were seen for the resonant frequencies (2.6 Hz vs. 2.8 Hz) and amplifications (8.0 vs. 9.5). In general, the fundamental frequency derived from earthquake signals tends to come very close to the fundamental frequency obtained from microtremors, whereas there is no clear correlation between amplification obtained from these two types of data, being in line with the result described by Duval et al. (2001). The clear peaks obtained from the two methods show a large impedance contrast

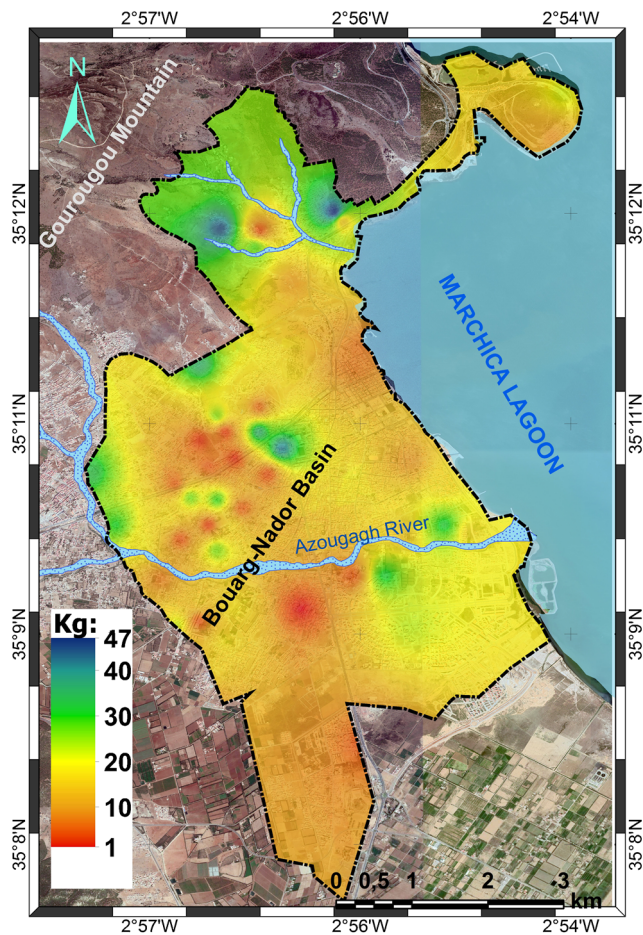


Fig. 14 Distribution of the vulnerability indices in the study area

between the sedimentary cover and the bedrock (Pilz et al. 2009).

Conclusion

This work constitutes a preliminary microzonation of the city of Nador. It provides fundamental frequencies, soil amplification, and ground vulnerability indices. Horizontal-to-vertical (H/V) measurements were used to quantify soil response, in a broader context of anticipating local seismic hazard. To this end, background noise recordings in the Nador urban area were analyzed, from more than 190 sites. An interpretation relative to the variations of the H/V spectral amplitude ratios in terms of local lithology is proposed.

The stability of the measurements was confirmed by records covering several months (September 2016 to August 2018) as well as some repeated measurements. The average fundamental frequencies obtained were identical at a given site under the same conditions of measurement. Accordingly, the predominant frequency in the urban area is between 1.1 and 4.8 Hz, with an amplification factor ranging from 2.5 to 11.4. The fundamental frequency obtained on the basis of a strong motion record in Nador was 2.6 Hz, with an amplification value near 8. In general, these values agree with the values from nearby microtremor measurements.

Amplification is observed in particular around the Azougagh River and, in some mountainous areas, in both cases, characterized by alluvium or river deposits. In some sites of the study area, we noted that amplification varies due to factors such as the composition of soil layers, whose density, velocity, and thickness appear to affect the impedance contrast.

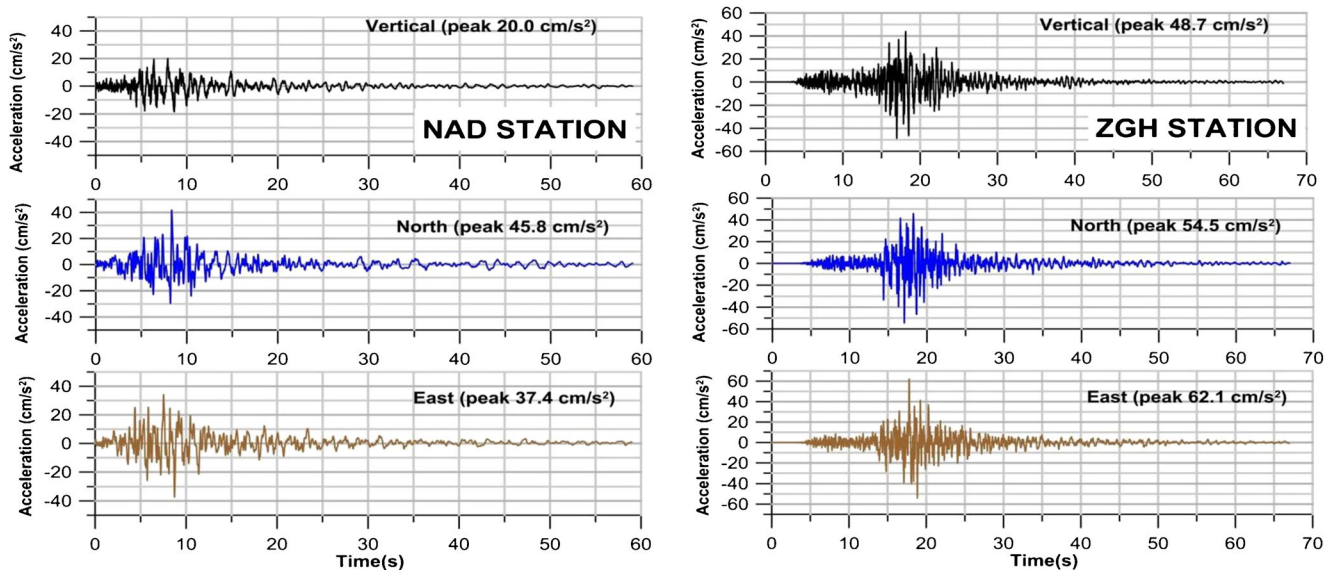
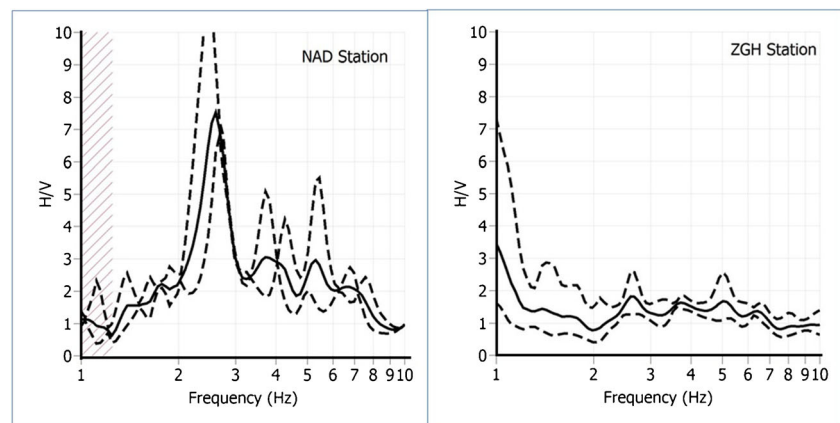


Fig. 15 Recorded acceleration at NAD and ZGH stations for the 25 January 2016, Alboran earthquake (6.3 MW)

Fig. 16 HVSR in NAD and ZGH stations



Envisaging its role in future seismic hazard assessment, the vulnerability index was also taken into account here. We obtained values between 1.3 and 43. Values above 20 indicate vulnerable areas that may present significant soil deformation during a seismic action. Such areas would be largely located at the foot of the Gourougou Mountain (to the west of the city) or near the river. This research furthermore points to the substantial influence of site effects in view of earthquake ground motion records. Given its soft and thick underlying sediments, the city is vulnerable to the phenomenon of amplification during a seismic action. It is advisable to improve upon this survey using further geophysical techniques, especially to determine the V_{S30} parameter. Arriving at more complete information on ground characteristics would be beneficial and relevant for urban planning and engineering undertakings in the region. In sum, the determination of parameters such as those provided here can amount to a valuable contribution in the

context of microzoning this seismic region in northeastern Africa.

Acknowledgements The authors are grateful to all staff of the Geological Department, in the Faculty of Sciences, Oujda. Our thanks to CNRST-Rabat for the information they provided for this work. We also express our gratitude to the reviewers, whose comments have substantially improved our original manuscript. This research was performed in the framework of a joint collaboration between the Geological Department of the University of Mohamed First, Oujda, Morocco, and the Department of Physics, University of Jaén, Spain.

Funding Partial funding came from Spain's Consejería de Economía, Conocimiento, Empresa y Universidad, under the Programa Operativo FEDER Andalucía 2014-2020—call made by the University of Jaén 2018.

Declarations

Conflict of interest The authors declare that they have no competing interests.

References

- Achalhi M (2016) Chronostratigraphie et sédimentologie des bassins néogènes de Boudinar et d'Arbaa Taourirt (Rif oriental, Maroc). Doctoral dissertation, Université Mohammed Premier
- Albarello D, Lunedei E (2010) Alternative interpretations of horizontal to vertical spectral ratios of ambient vibrations : new insights from theoretical modeling. *Bull Earthq Eng* 8:519–534. <https://doi.org/10.1007/S10518-009-9110-0>
- Ali A, Kim KY (2016) Seismic site conditions in Gangneung, Korea, based on Rayleigh-wave dispersion curves and topographic data. *Geosci J* 20:781–791. <https://doi.org/10.1007/S12303-016-0013-1>
- Ammar A, Mauffret A, Gorini C, Jabour H (2007) The tectonic structure of the Alboran Margin of Morocco. *Rev Soc Geol Esp* 20:247–272
- Anandarajah A, Rashidi H, Arulananadan K (1995) Elasto-plastic finite element analyses soil-structure system under earthquake excitations. *Comput Geotech* 17:301–325
- Bard P-Y (1995) Effects of surface geology on ground motion : recent results and remaining issues. In: 10th European Conference on Earthquake Engineering :305–323

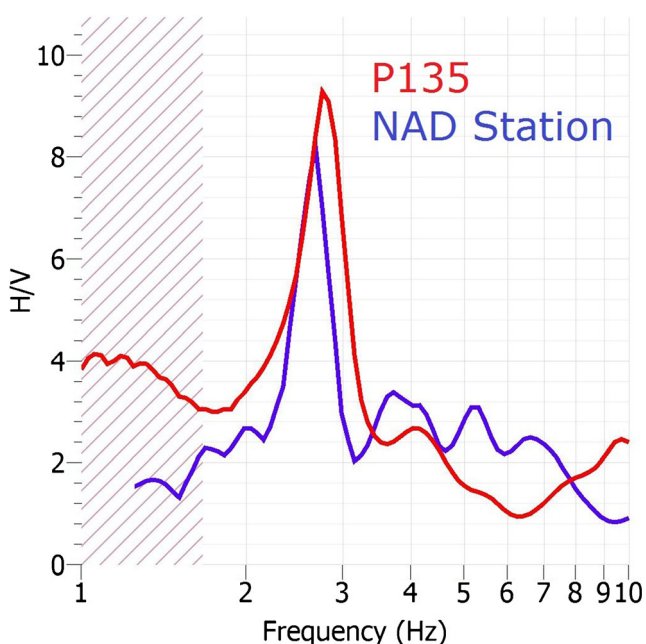


Fig. 17 Comparison of H/V spectral ratio from microtremors and H/V from earthquake motions at NAD station

- Bard P-Y (1999) Microtremor measurement : a tool for site effect estimation. *Eff Surf Geol Seism Motion* 3(june):1251–1279
- Bard P-Y, Duval A, Koehler A, Sandro R (2004) Guidelines for the implementation of the h/v spectral ratio technique on ambient vibrations measurements , processing and interpretation. *Bull Earthq Eng* 169(December):1–62. <https://doi.org/10.1111/J.1365-246x.2006.03282.X>
- Beskos DE (1987) Boundary Element Methods in Dynamic Analysis. *Appl Mech Rev* Vol 50:540
- Bindi D, Parolai S, Grosser H, Milkereit C, Durukal E (2007) Empirical ground-motion prediction equations for northwestern Turkey using the aftershocks of the 1999 Kocaeli earthquake. *Geophys Res Lett* 34:L08305. <https://doi.org/10.1029/2007GL029222>
- Bonilla LF, Steidl JH, Grant TL, Tumarkin AG, Ralph JA (1997) Site amplification in the San Fernando Valley, California : Variability of Site-Effect Estimation Using the S-Wave , Coda , and H/V Methods. *BSSA* 87(3):710–730
- Bonnefoy-Claudet S, Cotton F, Bard PY (2006) The nature of noise wavefield and its applications for site effects studies. a literature review. *Earth Sci Rev* 79(3–4):205–227. <https://doi.org/10.1016/j.earscirev.2006.07.004>
- Boore ND, Gibbs JF, Joyner WB, Tinsley JC, Ponti DJ (2003) Estimated ground motion from the 1994 Northridge, California, Earthquake at the site of the interstate 10 and La Cienega Boulevard Bridge Collapse, West Los Angeles, California. *BSSA* 93(6):737–2751
- Borcherdt RD (1970) Effects of local geology on ground motion near san francisco bay. *Seismol Soc Am Bull* 60(1):29–61
- Bouchelouh A, Rabah Bensalem A, Zaourar N, Machane D, Moulouel H, El Hadi O (2017) The miocene roof mapping using microtremor recording and electrical survey method in blida city. *Alger Pure Appl Geophys* 175:287–301. <https://doi.org/10.1007/S00024-017-1684-X>
- Buform E, Bezzeghoud M, Udias A, Pro C (2004) Seismic sources on the Iberia-African plate boundary and their tectonic implications. *Pure Appl Geophys* 161:623–646. <https://doi.org/10.1007/s00024-003-2466-1>
- Campell KW (1981) Near source attenuation of peak horizontal acceleration. *Bull Seismol Soc Am* 71:2039–2070
- Cherkaoui TE, El Hassani A (2012) Seismicity and seismic hazard in morocco 1901-2010. *Bull Inst Sci Sect Sci Terre* 34(1):45–55
- Daryono S, Sartohadi J, Dulbahri KSB (2009) Pengkajian Local Site Effect Di Graben Bantul Menggunakan Indeks Kerent Anan Seismik Berdasarkan Pengukuran Mikrotremor. *Jurnal Kebencanaan Indonesia* 2(2009)
- Delgado J, Casado CL, Alfaro P, Giner JJ, Estévez A (1998) Liquefaction potential in the Lower Segura river basin (South-East Spain). *Eng Geol* 49(1):61–79. [https://doi.org/10.1016/s0013-7952\(97\)00073-2](https://doi.org/10.1016/s0013-7952(97)00073-2)
- Delgado J, Lopez C, Giner J, Estevez A, Cuenca A, Molina S (2000) Microtremors as a geophysical exploration tool : applications and limitations. *Pure Appl Geophys* 157:1445–1462
- Douglas J (2001) A comprehensive worldwide summary of strong-motion attenuation relation ships for peak ground acceleration and spectral ordinates (1969-2000). ESEE Report No. 01-1, Imperial College of Science, Technology and Medicine, Civil Engineering Department, London
- Douglas J, Aochi H, Suhadolc P, Costa G (2007) The importance of crustal structure in explaining the observed uncertainties in ground motion estimation. *Bull Earthq Eng* 5(1):17–26
- Douiri A, Mourabit T, Cheddadi A, Chourak M, Louhibi S (2015) Coïncidences spectrales du bruit de fond entre sol et bâti existant dans la ville d'Imzouren. *Maroc J Mater Environ Sci* 6(2):366–376
- Duval AM, Bard PY, Lebrun B, Lacave-Lachet C, Riepl J, Hatzfeld D (2001) H/V technique for site response analysis. synthesis of data from various surveys. *Boll Geofis Teor Appl* 42(3–4):267–280
- El Bakkali S, Bourdier JL, Gourgaud A (1998) Characterisation and stratigraphy of Upper Miocene volcanoclastic marker beds in the Melilla-lower Kert Basin (eastern Rif, Morocco). *Comptes Rendus de l'Academie des Sciences Series IIA Earth and Planetary Science* 2(327):93–100
- Esper P, Tachibana E (1998) Lessons from the kobe earthquake. *Geohazard Eng Geology Geol Soc* 15:105–116. <https://doi.org/10.1144/GSL.ENG.1998.015.01.11>
- Faure-Muret A, Choubert G, Dahmani M, El Mouatani A, Horrenberger JC, Salem M (1992) Carte géologique du Maroc à 1/100 000–feuille Agadir Melloul. Notes et Mémoires 359
- Foti S, Parolai S, Albarello A, Picozzi M (2011) Application of surface-wave methods for seismic site characterization. *Surv Geophys* 32(6):777–825. <https://doi.org/10.1007/s10712-011-9134-2>
- Fukushima Y, Tanaka T (1990) A new attenuation relation for peak horizontal acceleration of strong earthquake ground motion in Japan. *Bull Seismol Soc Am* 80:757–783
- Groholski DR, Hashash YMA, Kim B, Musgrove M, Harmon J, Stewart JP (2016) Simplified model for small-strain nonlinearity and strength in 1d seismic site response analysis. *J Geotech Geoenviron* 04016042:1–14. [https://doi.org/10.1061/\(ASCE\)GT.1943-5606.0001496](https://doi.org/10.1061/(ASCE)GT.1943-5606.0001496)
- Gulkan P, Kalkan E (2002) Attenuation modeling of recent earthquakes in Turkey. *J Seismolog* 6:397–409. <https://doi.org/10.1023/A:1020087426440>
- Gulkan P, Kalkan E (2005) Discussion of the paper: an empirical attenuation relationship for Northwestern Turkey ground motion using a random effects approach. *Soil Dyn Earthq Eng* 25:889–891
- Guralp Systems (2017) www.guralp.com
- Haddouti K, Zerrouki M (2016) Le projet d 'aménagement urbain et touristique de marchica au nord -est du maroc : conflit et analyse. *GeoDec* 4:1–12
- Haghshenas E, Theodulidis N, Bard P-Y (2008) Empirical evaluation of microtremor H/V spectral ratio. *Bull Earthq Eng* 6:75–108. <https://doi.org/10.1007/s10518-007-9058-x>
- Hamdache M, Peláez JA, Yelles-Chauche AK (2004) The Algiers, Algeria earthquake (MW 6.8) of 21 May 2003: preliminary report. *Seismol Res Lett* 75:360–367
- Hamdache M, Peláez J A., Yelles-chaouche A, Monteiro R, Marques M, Castro M, Beldjoudi H, Kherroubi A (2019) A Preliminary Seismic Hazard Modelling in Northern Algeria. *Adv Sci Technol Innov*:231–235. <https://doi.org/10.1007/978-3-030-01656-2>
- Hamdullah L, Irmak TS, Güven IT (2017) Seismic vulnerability indices of ground for De ğ İrmendere Kocaeli. *Bull Eng Geol Environ* 78: 507–517. <https://doi.org/10.1007/s10064-017-1102-8>
- HCP (2017) Monographie de la province de nador, Morocco. <http://www.hcp.ma/region-oriental>
- Horike M, Boming Z, Hiroshi K (2001) Comparison of site response characteristics inferred from microtremors and earthquake shear waves. *B.S.S.A* 91(6):1526–1536. <https://doi.org/10.1785/0120000065>
- Iida M, Kawase H (2004) A Comprehensive interpretation of strong motions in the mexican volcanic belt. *Bull Seismol Soc Am* 94(2): 598–618
- Jarpe SP, Hutchings LJ, Hauk TF, Shakal AF (1989) Selected strong- and weak-motion data from the loma prieta earthquake sequence. *Seismol Res Lett* 60(4):167–176
- Kariche J, Meghraoui M, Timoulali Y (2018) The Al Hoceima earthquake sequence of 1994 , 2004 and 2016: Stress transfer and poroelasticity in the rif and alboran sea region. *Geophys J Int* 212: 42–53. <https://doi.org/10.1093/gji/ggx385>
- Konno K, Ohmachi T (1998) Ground-motion characteristics estimated from spectral ratio between horizontal and vertical components of microtremor. *Bull Seismol Soc Am* 88(1):228–241
- Koulali A, Ouazar D, Tahayt A, King RW, Vernant P, Reilinger RE, McClusky S, Mourabit T, Davila JM, Amraoui N (2011) New GPS constraints on active deformation along the africa – Iberia plate

- boundary. *Earth Planet Sci Lett* 308(1–2):211–217. <https://doi.org/10.1016/j.epsl.2011.05.048>
- Lachet C, Denis H, Pierre YB, Nikos T, Christos P, Alekos S (1996) Site Effects and microzonation in the city of Thessaloniki (Greece) Comparison of different approaches. *BSSA* 86(6):1692–1703. <https://doi.org/10.2138/am-2000-2-302>
- Lermo J, Francisco J, Chávez-García J (1994) Are microtremors useful in site response evaluation. *Bull Seismol Soc Am* 84(5):1350–1364
- Ma J, Dong L, Zhao G, Li X (2018) Qualitative method and case study for ground vibration of tunnels induced by fault-slip in underground mine. *Rock Mech Rock Eng* 52:1887–1901. <https://doi.org/10.1007/s00603-018-1631-x>
- Ma J, Dong L, Zhao G, Li X (2019) Ground motions induced by mining seismic events with different focal mechanisms. *Int Rock Mech Min Sci* 116:99–110
- Mayoral JM, Asimaki D, Tepalcapa S, Wood C, Roman-de Sancha A, Hutchinson T, Franke K, Montalva G (2019) Site effects in Mexico city basin: past and present. *Soil Dyn Earthq Eng* 121(February):369–382. <https://doi.org/10.1016/j.soildyn.2019.02.028>
- Mubin F, Nurcahya B E (2014) Frequency analysis and seismic vulnerability index by using nakamura methods for microzonation at prambanan temple and its surrounding area, Yogyakarta Province, Indonesia. *Atlantis Press, International Conference on Physics* no. Icp: 91–96
- Mucciarelli M (1998) Reliability and applicability of Nakamura's technique using microtremors: an experimental approach. *Eng J Earthq* 2:625–638. <https://doi.org/10.1080/13632469809350337>
- Mucciarelli M (2008) Reliability and applicability of Nakamura's technique using microtremors: an experimental approach. *J Earthq Eng* 2(4):625–638. <https://doi.org/10.1080/13632469809350337>
- Mucciarelli M, Gallipoli MR (2004) The HVSR technique from microtremor to strong motion: empirical and statistical considerations. In *Proc. of 13th World Conference of Earthquake Engineering*, Vancouver, BC, Canada, paper (Vol. 45)
- Nakamura Y (1989) A method for dynamic characteristics estimation of subsurface using microtremor on the ground surface. *Quarterly Report of Railway Tech. Res Inst* 30(1):25–33
- Nakamura Y (1997) Seismic vulnerability indices for ground and structures using microtremor. *World Congress on Railway Research*, Florence, Nov. 1997(1): 1–7
- Nakamura, Y (2008) On the H/V spectrum. *World Conference on Earthquake Engineering*. 1–10
- Nakhcha C, Ait Brahim L, Chaoui A, Jabrane R, Elhammichi F, Tabyaoui H (2005-2006) *Aléa sismique du rif oriental et son avant-pays*. *Geomaghreb* 3:1–12
- Narayan JP (2010) Effects of impedance contrast and soil thickness on basin-transduced rayleigh waves and associated differential ground motion. *Pure Appl Geophys* 167(12):1485–1510. <https://doi.org/10.1007/s00024-010-0131-z>
- Nogoshi M, Igarashi T (1970) On the propagation characteristics of microtremor. *J Seism Soc Jpn* 23:264–280. https://doi.org/10.4294/zisin1948.23.4_264
- Panou AA, Theodulidis N, Hatzidimitriou P, Stylianidis K, Papazachos CB (2005a) Ambient noise horizontal-to-vertical spectral ratio in site effects estimation and correlation with seismic damage distribution in urban environment: the case of the city of Thessaloniki (Northern Greece). *Soil Dyn Earthq Eng* 25(4):261–274. <https://doi.org/10.1016/j.soildyn.2005.02.004>
- Panou AA, Papazachos CB, Theodulidis PM, Hatzidimitriou S (2005b) Reliability of ambient noise horizontal-to-vertical spectral ratio in urban environments : the case of Thessaloniki City (Northern Greece). *Pure Appl Geophys* 162:891–912. <https://doi.org/10.1007/s00024-004-2647-6>
- Park D, Hashash YMA (2008) Rate-dependent soil behavior in seismic site response analysis. *Can Geotech J. no. April*. <https://doi.org/10.1139/T07-090>
- Parolai S (2012) Investigation of site response in urban areas by using earthquake data and seismic noise. *GFZ Ger Res Cent Geosci*:1–34. <https://doi.org/10.2312/GFZ.NMSOP-2>
- Peláez JA, Chourak M, Tadili BA, Ait Brahim L, Hamdache M, López Casado C, Martínez Solares JM (2007) A catalog of main moroccan earthquakes from 1045 to 2005. *Seismol Res Lett* 78(6):614–621. <https://doi.org/10.1785/gssrl.78.6.614>
- Pilz M, Parolai S, Leyton F, Campos J, Zschau J (2009) A comparison of site response techniques using earthquake data and ambient seismic noise analysis in the large urban areas of Santiago de Chile. *Geophys J Int* 178(2):713–728. <https://doi.org/10.1111/j.1365-246X.2009.04195.x>
- Poggi V, Fäh D (2016) Guidelines and strategies for seismic microzonation in Switzerland. <https://doi.org/10.3929/ethz-a-010735479>
- Rathje EM, Jonathan P, Stewart M, Bora B, Jonathan DB, Bardet P (2006) Strong ground motions and damage patterns from the 1999 duzce earthquake in Turkey. *J Earthq Eng* 10(5):693–724
- Reglement Parasismique RPS (2000) Université Mohammed V Ministère de l'Habitat, de l'Urbanisme et de l'Aménagement de l'Espace, Direction Technique de L'Habitat. (2011). Version Révisée 2011
- Rosa-Cintas S, Clavero D, Delgado J, Garrido J (2017) Characterization of the shear wave velocity in the metropolitan area of Málaga (S Spain) using the H/V Technique. *Soil Dyn Earthq Eng* 92:433–442. <https://doi.org/10.1016/j.soildyn.2016.10.016>
- Satoh T, Kawase H, Matsushima S (2001) Differences between site characteristics obtained from microtremors, S-Waves, P-Waves, and Coda. *B.S.S.A* 91(2):313–334. <https://doi.org/10.1785/0119990149>
- Semblat J, Duval A, Dangla P (2000) Numerical analysis of seismic wave amplification in nice (France) and comparisons with experiments. *Soil Dyn Earthq Eng* 19:347–362
- Shapiro NM, Campillo M, Paul A, Singh SK, Jongmans D (1997) Surface-wave propagation across the Mexican volcanic belt and the origin of the long-period seismic-wave amplification in the valley of Mexico. *Geophys J* 128:151–166
- Singh SK, Ordaz M (1993) On the origin of long coda observed in the lake-bed strong-motion records of Mexico City. *BSSA* 83(3):1298–1306. https://doi.org/10.4294/zisin1948.23.4_264
- Strollo A, Parolai S, Bindi D, Chiauzzi RP, Mucciarelli M, Jochen Z (2011) Microzonation of Potenza (Southern Italy) in terms of spectral intensity ratio using joint analysis of earthquakes and ambient noise. *Bull Earthq Eng* 10(2):493–516. <https://doi.org/10.1007/s10518-011-9256-4>
- Sunaryo S (2017) Study of seismic vulnerability index (Kg) from dominant frequency (f0) and amplification factor (A0) by means of microzonation Data: Conference: 2017 International Seminar on Sensors, Instrumentation, Measurement and Metrology (ISSIMM) 78–81. 10.1109/ISSIMM.2017.8124266
- Takekawa I (1998) Remarkable response amplification of building frames due to resonance with the surface ground. *Soil Dyn Earthq Eng* 17(4):211–218
- Talhaoui A, Iben'brahim A, Aberkan M, Kasmi M, El. Mouraouah A (2004) Seismic microzonation and site effects at al Hoceima city, Morocco. *J Earthq Eng* 8(4):585–596. <https://doi.org/10.1080/13632460409350502>
- Trifunac MD, Todorovska MI (1997) Northridge, California, earthquake of 1994: density of pipe breaks and surface strains. *Soil Dyn Earthq Eng* 16:193–207. [https://doi.org/10.1016/S0267-7261\(96\)00042-5](https://doi.org/10.1016/S0267-7261(96)00042-5)
- Ulutaş E, Özer MF (2010) Empirical attenuation relationship of peak ground acceleration for Eastern Marmara region in Turkey. *Arab J Sci Eng* 35:187–203
- Ulutaş E, Coruk Ö, Karakaş A (2011) A study of residuals for strong ground motions in Adapazari basin, NW Turkey, by ground motion prediction equations (GMPEs). *Stud Geophys Geod* 55(2):213–240

- Upadhyay B, Mori S (2013) Comparison of H / V Ratios and predominant frequencies inferred from microtremors and earthquake motions in Ehime Prefecture. Japan 1:117–118
- Youd TL, Perkins DM (1978) Mapping liquefaction-induced ground failure potential. J Geotech Eng Div 104:13659
- Zaslavsky Y, Ataev G, Gorstein M, Kalmanovich M, Hofstetter A, Perelman N et al (2008) Microzoning of site response parameters in the towns of Dimona and bet Shean (Israel). Bollettino di Geofisica, teorica and applicata 49(1):109–130